Discrete Ridgelet transform: application to the denoising of color images

Philippe Carré and Eric Andres
IRCOM-SIC Laboratory, UMR CNRS 6615
BP 30179, 86962 Futuroscope, France

Abstract

In this paper we present a new discrete implementation of ridgelet transforms based on Reveillès discrete 2D lines. Ridgelet transforms are particular invertible wavelet transforms. Our approach uses the arithmetical thickness parameter of Reveillès lines to adapt the Ridgelet transform to specific applications. We illustrate this with a color denoising algorithm. The broader aim of this paper is to show how results of discrete analytical geometry can be sucessfully used in color image analysis.

1. Introduction

Image analysis is traditionally aimed at understanding digital signals obtained by sensors (in our case cameras). Digital information is considered as sampled continuous information and the theoretical background for it is signal theory. This is sometimes referred to as *"digital geometry"* in opposition to *"discrete geometry"* for computer graphics. These last ten years, since J-P. Reveillès has introduced it [6], *discrete analytical geometry* has made an important progress in defining and studying classes of discrete objects and transformations. This greatly enhanced our understanding of the links between the discrete world $\mathbb{Z}^{\aleph}$ and the continuous world $\mathbb{R}^{\aleph}$. In the same time, a new discrete signal decomposition has been developed in image analysis: the wavelet representation. This new representation has many applications such as denoising, compression, analysis, etc. One of the aims of this paper is to apply this new insight in discrete geometry to image analysis and more specifically to a particular wavelet transform: the ridgelet transform.

Wavelets are very good at representing point singularities ; however they are significantly less efficient when it comes to linear singularities. Because edges are a extremely common phenomena in natural images, an efficient multiresolution representation of images with edges would be quite advantageous in a number of applications. A team of Stanford has recently developed an alternative system of multiresolution analysis specifically designed to efficiently represent edges in images [2]. Their attempt was to design a new system, called ridgelet transform, in the continuous domain so that an image could be approximated within a certain margin error with significantly fewer coefficients than would be required after a wavelet decomposition. However, most of the work done with ridgelets has been theorical in nature and discussed in the context of continuous functions. The important bridge to digital implementation is tenuous at best. To our knowledge, we can find in the literature only two solutions for the digital ridgelet decomposition [4], [7] (notice that the study proposed by Guédon et al is similar [5]).This paper presents a new approach that aims at representing linear singularities with a discrete ridgelet transform based on Reveillès discrete lines.

In this article, we propose a new approach of the ridgelet transform based on several types of Reveillès discrete lines definitions in the Fourier domain. Our decomposition has an exact inverse reconstruction process and the redundancy of our Ridgelet representation can be adjusted with the arithmetical thickness of the Reveilles discrete lines. To illustrate this new decomposition, we propose a method of restoration of noised images which uses a wavelet undecimated method defined in [3].

2. The wavelet transform

The discrete wavelet transform (DWT) stems from the multiresolution analysis and filter bank theory. The wavelet analysis is defined as:

$$\begin{aligned} c_l(k) &= \frac{1}{\sqrt{2}} \sum_n h(n-2k)\, c_{l-1}(k),\ d_l(k) \\ &= \frac{1}{\sqrt{2}} \sum_n g(n-2k)\, c_{l-1}(k) \end{aligned} \tag{1}$$

with c_l the coarse approximation and d_l the decimated wavelet coefficients at scale l and c_0 the original signal. The sequence $\{h(k), k \in Z\}$ is the impulse response of a low-pass filter. The sequence $\{g(k), k \in Z\}$ is the impulse response of a high-pass filter. Notice that with conditions required on the filters, we get an exact restoration.

Because of decimation, the Mallat's decomposition is completely time variant. A way to obtain a time-invariant

system is to compute all the integer shifts of the signal. Since the decomposition is not decimated, filters are dilated between each projection. This algorithm presents many advantages, particulary a knowledge of all wavelets' coefficients: coefficients removed during the downsampling are not necessary for a perfect reconstruction, but they may contain information useful for the denoising.

3. The ridgelet transform

3.1. Continuous theory

A substantial foundation for Ridgelet analysis is documented in the Ph.D. thesis of Candès [2]. We briefly review the ridglet transform and illustrate its connections with the radon and wavelet transforms in the continuous domain. The continuous ridgelet transform of $s \in L^2\left(\Re^2\right)$ is defined by :

$$r(a,b,\theta) = \int_{R^2} \psi_{a,b,\theta}(\mathbf{x})\mathbf{s}(\mathbf{x})\mathbf{dx}$$

with $\psi_{a,b,\theta}(\mathbf{x})$ the ridglet 2-D function defined from a wavelet 1-D function ψ as:

$$\psi_{a,b,\theta}(\mathbf{x}) = \mathbf{a}^{-\mathbf{1/2}}\psi\left(\frac{\mathbf{x_1}\cos\theta + \mathbf{x_2}\sin\theta - \mathbf{b}}{\mathbf{a}}\right)$$

b is the translation parameter, a is the dilatation parameter and θ is the direction parameter.

The function is oriented at the angle θ and is constant along lines $x_1\cos\theta + x_2\sin\theta = cst$. Transverse to these ridges it is a wavelet. In comparison, the analysis continuous 2-D wavelet function are tensor products of 1-D wavelet $\psi_{a,b}$:

$$\psi_{\mathbf{a},\mathbf{b}}(\mathbf{x}) = \psi_{\mathbf{a_1},\mathbf{b_1}}(\mathbf{x_1})\psi_{\mathbf{a_2},\mathbf{b_2}}(\mathbf{x_2})$$

The Radon transform seems to be similar to the 2-D wavelet transform but the translation parameters (b_1, b_2) are replaced by the line parameters (b,θ). Then, the wavelets are adapted to analyse isolated point discontinuities, while the ridgelets are adapted to analyse discontinuities along lines.

A basic tool for calculating ridgelet coefficients is to view ridgelet analysis as a form of wavelet analysis in the Radon domain: in 2-D, points and lines are related via the radon transform, thus the wavelet and ridgelet transforms are linked via the Radon transform.

The Radon transform of s is defined as:

$$Rs(\theta,t) = \int_{R^2} s(\mathbf{x})\delta(\mathbf{x_1}\cos\theta + \mathbf{x_2}\sin\theta - \mathbf{t})\mathbf{dx_1dx_2}$$

where δ is the Dirac distribution. The ridgelet coefficients $r(a,b,\theta)$ of s are given by the 1-D wavelet transform to the projections of the Radon transform where the direction θ is constant and x is varying:

$$r(a,b,\theta) = \int_R \psi_{a,b}(x)Rs(\theta,x)dx$$

Notice that the Radon transform can be obtained by applying the 1-D inverse Fourier transform to the 2-D Fourier transform restricted to radial lines going through the origin (this is exactly what we are going to do in the discrete Fourier domain with help of discrete Reveillès lines):

$$\widehat{s}(\omega\cos\theta, \omega\sin\theta) = \int_R e^{-j\omega x}Rs(\theta,x)dx$$

with $\widehat{s}(\omega)$ the 2-D Fourier transform of s.

This is the projection-slice formula which is used in image reconstruction from projection methods. We deduce that the Radon transform can be obtained by appying the 1-D inverse Fourier transform to the 2-D Fourier transform restricted to radial lines going through the origin.

3.2. Digital Ridgelet Transform

As we have seen, a basic strategy for calculating the continuous ridgelet transform is first to compute the Radon transform $Rs(\theta,t)$ and secondly, to apply a 1-D wavelet transform to the slices $Rs(\theta,.)$. The discrete procedure uses the same principle.

As presented in the first section, the discrete wavelet decomposition is easy to implement, is stable and invertible, and can be associated to a discrete orthogonal representation.

The discretization of the Radon transform is more difficult to achieve. The majority of methods proposed in the literature have been devised to approximate the continuous formula. But, none of them were specifically designed to be invertible transforms for discrete images and can not be used for the discrete Ridgelet transform. Recently, some articles studied the implementation of the digital Ridgelet transform. Two approaches have been developed:

- Spatial strategy for digital Radon transform: the Radon transform is defined as summations of image pixels over a certain set of lines. Those lines are defined in a finite geometry in a similar way as the line for the continuous Radon transform in the Euclidean geometry.

  $$Rs(p,q,b) = \sum_x \sum_y s(x,y)\delta\left(b + px - qy\right)$$

  with (p,q) direction of projection

  In [5] an inverse transform based on erosion and dilatation operations is proposed. Vetterli et al. proposed in [4] an orthonormal ridgelet transform.

- Fourier strategy for digital Radon transform: the projection slice formula suggests that approximate Radon transforms for digital data can be based on discrete Fast Fourier transforms (FFT). This is a widely used approach in the literature of medical imaging and synthetic aperture radar imaging. The Fourier-domain computation of an approximate digital radon transform is defined as:

  1. Compute the 2-D FFT of f
  2. Extract Fourier coefficients which fall lines L_θ going through the origin.
  3. Compute the 1-D FFT on each line L_θ (defined for each value of the angular parameter).

  In this strategy too, discrete lines must be defined. In [7], Starck et Al proposed to use an interpolation scheme which substitutes the sampled value of the Fourier transform obtained on the square lattice with sampled value of $\widehat{s}$ on a polar lattice. In this paper, we propose to define the lines L_θ with the discrete geometry in the Fourier domain. This solution allows us to have different Ridgelet decompositions according to the arithmetical thickness of the discrete Reveillès lines. Our transformation is redundant but the repetition of information depends on the type of the discrete lines used and can be adapted with the application. Moreover we obtain an exact reconstruction.

4. Digital Radon transform based on Reveillès discrete 2D lines

4.1. Definition of discrete lines

The discrete lines that are used in our application are not classical discrete lines such as, for instance, Bresenham lines nor the classical Reveillès lines. These lines are not suitable for our purpose because they do not provide a central symmetry in the Fourier domain. Without central symmetry, the inverse Fourier transform would produce imaginery values during the Radon transform. Central symmetry is obtained easily by using closed Reveillès discrete lines defined as follows:

$$L^{\omega}_{(p,q)} = \left\{ (x,y) \in Z^2 \, | |px+qy| \leq \omega/2 \right\}$$

with $(p,q) \in \mathbb{Z}^{\not\Subset}$ the direction of the line (direction of Radon projection) and ω the arithmetical thickness.

The parameter ω defines the connectivity of the discrete lines. The closed discrete lines have many interesting properties. One of the most important ones is that each type of closed discrete line is directly linked to a distance: for instance

$$L^{\sqrt{p^2+q^2}}_{(p,q)} = \left\{ (x,y) \in Z^2 \, \middle| \, |px+qy| \leq \frac{\sqrt{p^2+q^2}}{2} \right\}$$

is equal to $\left\{ M \in Z^2 \, \middle| d_2\left(M, L_{(p,q)}\right) \leq \frac{1}{2} \right\}$ where $L_{(p,q)}$: $px+qy=0$ is the Euclidean line of direction (p,q) and d_2 the Euclidean distance [1].

4.2. Closed Reveillès discrete lines for digital Radon transform

Our Digital Radon transform is defined by:

$$R^{\omega}s(p,q,b) = \sum_{k=0}^{K} \widehat{s}(\mathbf{f_k}) \mathrm{e}^{\mathbf{2\pi j \frac{k}{K} b}}$$

$$\text{with } \mathbf{f_k} = \begin{pmatrix} f_1^k \\ f_2^k \end{pmatrix} \text{ such that } \left| pf_1^k + qf_2^k \right| \leq \omega/2$$

$$\text{and } K \text{ length of a line segment of } L^{\omega}_{p,q}$$

We must define the set of discrete directions (p,q) in order to provide a complete representation. The set of line segments must cover all the square lattice in Fourier domain. For this, we define the direction (p,q) according to pairs of symmetric points from the boundary of the 2-D Discrete Fourier Spectra.

Proposition 1 *Let a square lattice be defined as* $\Omega_N^2 = [-N,N] \times [-N,N]$. *Let us consider the set of directions* (p_m, q_m) *with, for* $0 \leq m \leq 2N$, $(p_m, q_m) = (N, m-N)$ *and for* $2N+1 \leq m \leq 4N-2$, $(p_m, q_m) = (m-3N+1, N)$. *The set of all the closed lines defined by* $|p_m f_1 + q_m f_2| \leq \omega_m/2$ *with* $\omega_m \geq \sup(|p_m|, |q_m|)$ *provides a complete cover of the lattice* Ω_N^2.

The proof of this proposition is obvious because of a well known result in discrete analytical geometry that states that a closed discrete line of direction (p,q) is connected if and only if $\omega \geq \sup(|p|,|q|)$ [6]. For thinner (non connected) discrete lines, with values of $\omega < \sup(|p|,|q|)$, it is possible but not certain that we also achieve a complete cover of the lattice Ω_N^2 depending on the value of ω compared to N. however, for our applications, we prefered working with connected discrete lines.

Three different types of closed discrete lines have been tested:

- closed naïve discrete lines: $\omega = \sup(|p|,|q|)$. These lines are the thinnest connected closed discrete lines. They are 8-connected. They provide therefore the

smallest redundancy. Closed naïve discrete lines are reated to the distance

$$d_1 : L_{(p,q)}^{\sup(|p|,|q|)} = \left\{ M \in Z^2 \left| d_1\left(M, L_{(p,q)}\right) \leq \frac{1}{2} \right. \right\}$$

where $d_1(A,B) = |x_A - x_B| + |y_A - y_B|$;

- supercover lines: $\omega = |p| + |q|$. These lines are the thickest connected closed discrete lines that have been considered in our applications. They are the thinnest closed lines that are 4-connected and that cover the Euclidean line they approximate. They provide of course an important redudancy. Supercover lines are related to the distance d_∞:

$$L_{(p,q)}^{|p|+|q|} = \left\{ M \in Z^2 \left| d_\infty\left(M, L_{(p,q)}\right) \leq \frac{1}{2} \right. \right\}$$

  The supercover lines have an important theoretical importance.

- closed pythagoricean lines: $\omega = \sqrt{p^2+q^2}$. These lines are 8-connected and offer a medium redundancy, in between the naïve and supercover lines. The lines are related to the Euclidean distance d_2:

$$L_{(p,q)}^{\sqrt{p^2+q^2}} = \left\{ M \in Z^2 \left| d_2\left(M, L_{(p,q)}\right) \leq \frac{1}{2} \right. \right\}$$

  These lines possess the property of having a number of pixels per period close to its length. This means, in practice, that if pixels of the discrete line would hold energy, this energy would be distributed evenly along the line in the same way independently of the slope of the line.

4.3. Discrete Ridgelet transform

Now, to obtain the Ridgelet transform, we simply apply the 1-D wavelet transform on each discrete Radon coefficients $R^\omega s(p,q,b)$ obtained on the line segment $L_{p,q}^\omega$.

This transform is easily invertible. The reconstruction procedure works as follows:

1. Compute the inverse 1-D wavelet transform followed by the inverse 1-D FFT transform for each set

$$R^\omega s(p_m, q_m, .)$$

   with $m \in [0, 4N-2]$

2. Substitue the sampled value of $\widehat{f}$ on the lattice where the points fall on lines $L_{p,q}^\omega$ with the sampled value of $\widehat{f}$ on the square lattice.

The precedent procedure permits one to obtain an exact reconstruction if the set of $M = 4N-2$ lines provides a complete cover of the square lattice.

Now with our invertible discrete Radon transform, we can obtain an invertible discrete Ridgelet transform by taking the discrete wavelet transform on each Radon projection sequence

$$\{R^\omega s(p_m, q_m, k)\}_{b \in [0, K-1]}$$

where the direction (p_m, q_m) is fixed. This wavelet transform can be decimated or undecimated and the wavelet base can be adapted according to the application, as for the classical wavelet decomposition.

5. Denoising of color images by Ridgelet transform

We can generalize to color images the discrete wavelet decomposition presented in the first section. For this, we apply convolutions on the three components of the color image. With the same strategy, we can compute the Radon transform on the three components. But we must select an adapted color space. For the denoising application, we choose the YC_rC_b space, to treat separately the color and intensity components.

The procedure of denoise by Ridgelet transform is simply to perform thresholding on the Ridglet coefficients and compute the inverse Ridgelet transform. To perform thresholding, we use our undecimated method developed for the wavelet decomposition [3]. The redundance of the wavelet decomposition, associated with this method, reduces artifacts which appear after thresholding.

We present in the figure two results of our denoising method. With the first example, we can see that this method can reconstruct very noisy image. Because of the adaptation of this decomposition to linear singularities, the edges of objects are keeping and the noise seems to be removed. The second example illustrates the results for different definition of the lines $L_{p,q}^D$. As for the first image, the features are generally correctly reconstructed and the noise is smoothed. But if we study more precisely the result on the woman's hat, we see that the denoising is better for $D = \frac{|p|+|q|+1}{2}$ than for $D = \frac{\max(|p|,|q|)}{2}$. The first choice of D introduces more redundancy into the decomposition and thus reduces artifacts.

This new decomposition can be adapted to others noisy images by using others color spaces, discrete lines and wavelet bases. More generally, many applications can use this decomposition : for example, with a parameter D correctly chosen, we can limit the redundancy of the decomposition and thus use the representation for a compression

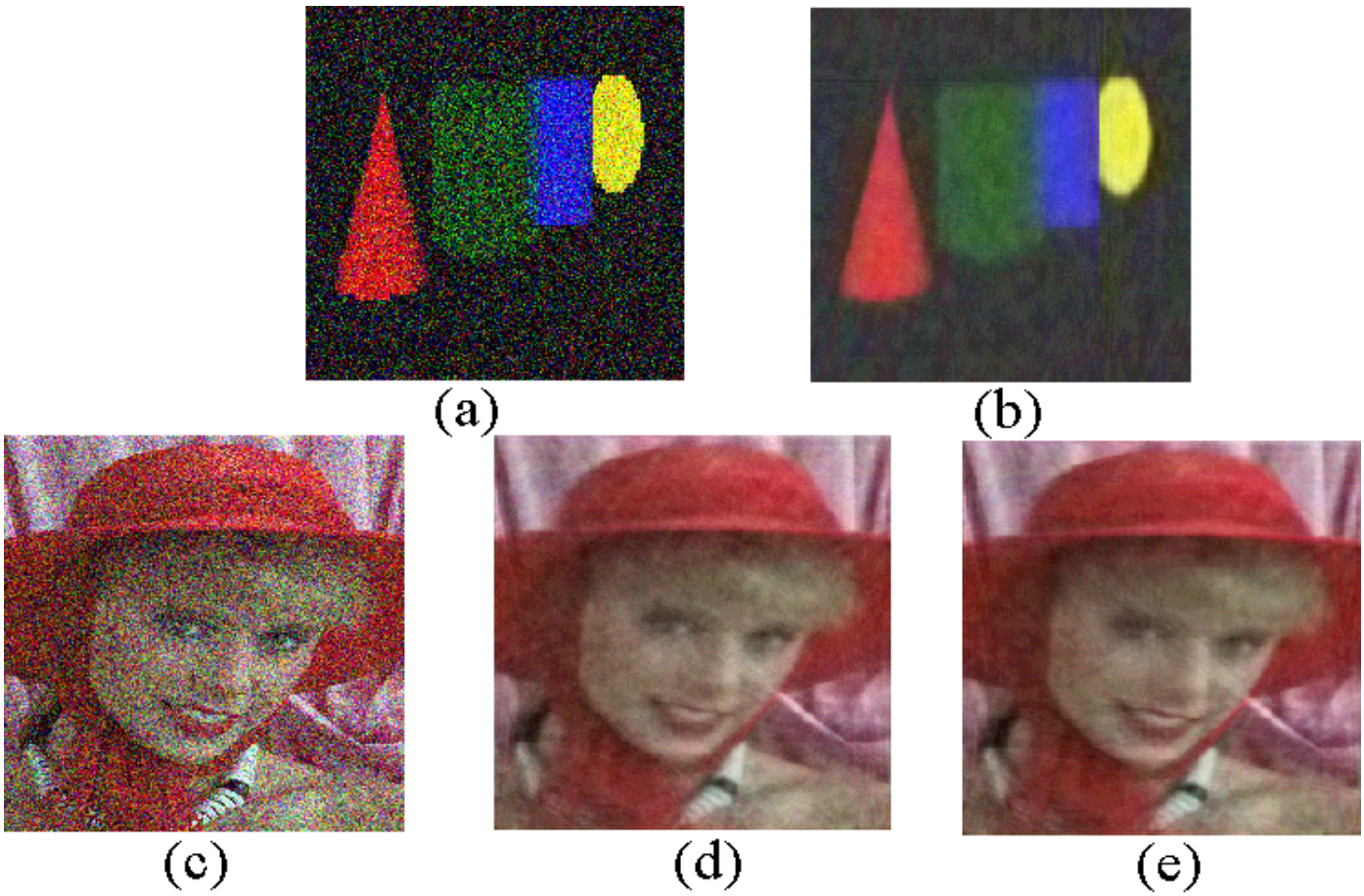

Figure 1: *(a) noisy image "object" (b) denoised by ridglet decomposition with* $D = \frac{\sqrt{q^2+p^2}}{2}$ *(c) noisy image woman (d) denoised by ridglet decomposition with* $D = \frac{\max(|p|,|q|)}{2}$ *(e) denoised by ridglet decomposition with* $D = \frac{|p|+|q|+1}{2}$

algorithm with a selection of the largest Ridglet coefficients.

References

[1] Eric Andrès. Modélisation analytique discrète d'objets géométriques. Habilitation, Université de Poitiers, 2000.

[2] E. Candès. *Ridgelets: Theory and Applications*. PhD thesis, Stanford, 1998.

[3] P. Carré, H. Leman, C. Marque, and C. Fernandez. Denoising the EHG signal with an undecimated wavelet transform. *IEEE Trans. on Biomedical Engineering*, 45(8):1104–1113, September 1998.

[4] M. Do and M. Vetterli. Discrete ridgelet transforms for image representation. Submitted to IEEE Trans. on Image Processing, April 2001.

[5] N. Normand and P. Guedon. Transformee mojette : une transformee redondante pour l'image. *Compte rendu de l'Académie des Sciences*, 1998.

[6] Jean-Pierre Reveillès. Géométrie discrète, calcul en nombres entiers et algorithmique. Habilitation, Université Louis Pasteur de Strasbourg, 1991.

[7] J. L. Starck, E. J. Candès, and D. L. Donoho. The curvelet transform for image denoising. Technical report, Department of Statistics, Stanford, November 2000.